

pubs.acs.org/JACS Communication

# Homologation of Electron-Rich Benzyl Bromide Derivatives via Diazo C—C Bond Insertion

Atanu Modak, Juan V. Alegre-Requena, Louis de Lescure, Kathryn J. Rynders, Robert S. Paton,\* and Nicholas J. Race\*



Cite This: https://doi.org/10.1021/jacs.1c11503



**ACCESS** 

III Metrics & More

Article Recommendations

Supporting Information

**ABSTRACT:** The ability to manipulate C–C bonds for selective chemical transformations is challenging and represents a growing area of research. Here, we report a formal insertion of diazo compounds into the "unactivated" C–C bond of benzyl bromide derivatives catalyzed by a simple Lewis acid. The homologation reaction proceeds via the intermediacy of a phenonium ion, and the products contain benzylic quaternary centers and an alkyl bromide amenable to further derivatization. Computational analysis provides critical insight into the reaction mechanism, in particular the key selectivity-determining step.

Synthetic approaches to organic compounds are grounded in the combination of nucleophiles and electrophiles.<sup>1</sup> For example, benzyl halide derivatives may participate in classical reactions such as nucleophilic substitution and electrophilic aromatic substitution (Figure 1A).<sup>2</sup> The advent of reactions that unlock "nonclassical" transformations of common building blocks provides opportunities to reimagine and/or streamline synthetic strategies. "Nonclassical" reactions may be described as those reacting at a traditionally inert functionality, for example, insertion into the  $C(sp^2)-C(sp^3)$  bond of a benzyl halide derivative (Figure 1B). Cascade reactions that effect formal C-C bond insertion reactions via skeletal rearrangements represent an appealing approach toward such a goal. 3,4 Herein, we describe the development of a homologation reaction of electron-rich benzyl bromide derivatives involving formal insertion of diazo compounds into the  $C(sp^2)-C(sp^3)$ bond (Figure 1C).

Cognizant of the ionic reactivity of diazo compounds with sp<sup>2</sup>-hybridized electrophiles (e.g., carbonyl derivatives),<sup>6</sup> we questioned whether electron-rich benzyl bromide A would react with diazo B, via the intermediacy of a stabilized benzylic carbocation, to generate alkyl diazonium ion C (Figure 1C). Loss of nitrogen would then trigger neighboring group participation of the aryl ring, resulting in phenonium ion D. 8,9 The bromide leaving group from the first step could then engage the putative spirocyclopropane at the less substituted position to afford the desired product E. 10 Tertiary bromide F was considered a potential side product accessible via competitive intermolecular displacement of nitrogen in diazonium C or nucleophilic opening of phenonium ion D at the more substituted position. The desired product E contains an acyclic, benzylic tertiary or quaternary center-motifs present in many pharmaceutical and agrochemical molecules (Figure 1D)<sup>11,12</sup>—while retaining the alkyl bromide as a functional handle for further derivatization. <sup>13,14</sup> This method enables programmable introduction of trifluoromethyl, ester, amide, ketone, and sulfone functional groups via a unified approach. In particular, the incorporation of trifluoromethyl

groups into molecules continues to be important in medicinal chemistry, <sup>15</sup> and the use of substituted trifluoromethyl diazo derivatives is particularly underexplored in this regard. <sup>16</sup>

4-Methoxybenzyl bromide 1 and trifluoromethyl diazo 2 were chosen as parent substrates for reaction discovery and optimization. After surveying a series of Lewis acids under different reaction conditions, it was found that SnBr<sub>4</sub> (50 mol %) in  $CH_2Cl_2$  at -78 °C afforded bromide 3a in 75% isolated yield (Figure 2A).<sup>17</sup> With the optimized conditions in hand, the scope of the reaction was evaluated with respect to both substituents on the diazo and the benzyl bromide derivative. Several different electron-withdrawing groups worked well in this process (Figure 2A). Alkyl-substituted diazo derivatives containing an ethyl ester (3b), benzyl ester (3c), redox-active ester (3d), and a nitrile (3e) were all effective in this reaction. With ester derivatives, minor quantities of isomer 3' are observed in the <sup>1</sup>H NMR spectrum of the crude reaction mixture. For completeness, the ratio of 3:3' in the isolated material is quoted in parentheses, and the ratio in the crude reaction mixture is quoted in brackets below. The use of monosubstituted diazo derivatives to generate tertiary benzylic centers is also possible and further highlights the range of electron-withdrawing substituents amenable in this reaction (Figure 2B). An ethyl ester (3f), benzyl ester (3g), tert-butyl ester (3h), amide (3i), ketone (3j), trifluoromethyl group (3k), and a sulfone (3l) all worked well to give the requisite tertiary benzylic centers.

Trifluoromethyl-substituted diazo 2 was employed to evaluate a number of electron-rich benzyl bromide derivatives in the homologation reaction (Figure 2C). In all cases, the

Received: October 31, 2021



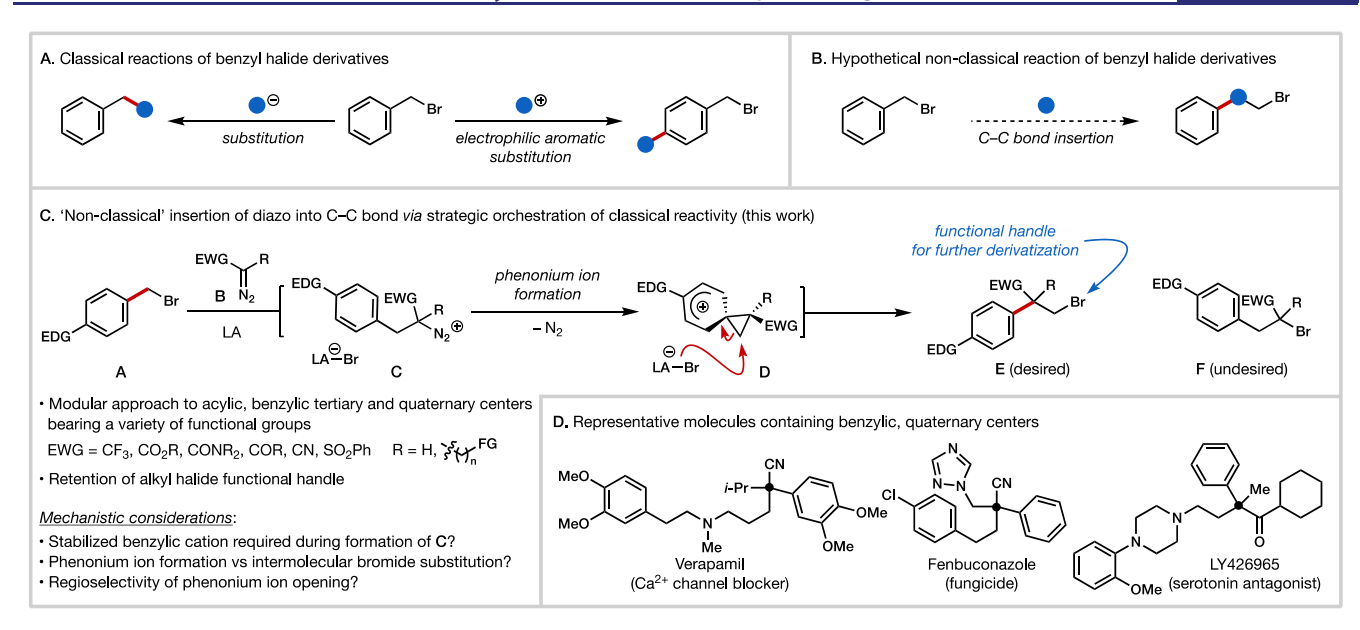


Figure 1. Nonclassical insertion of diazo compounds into C-C bond of benzyl bromide derivatives.

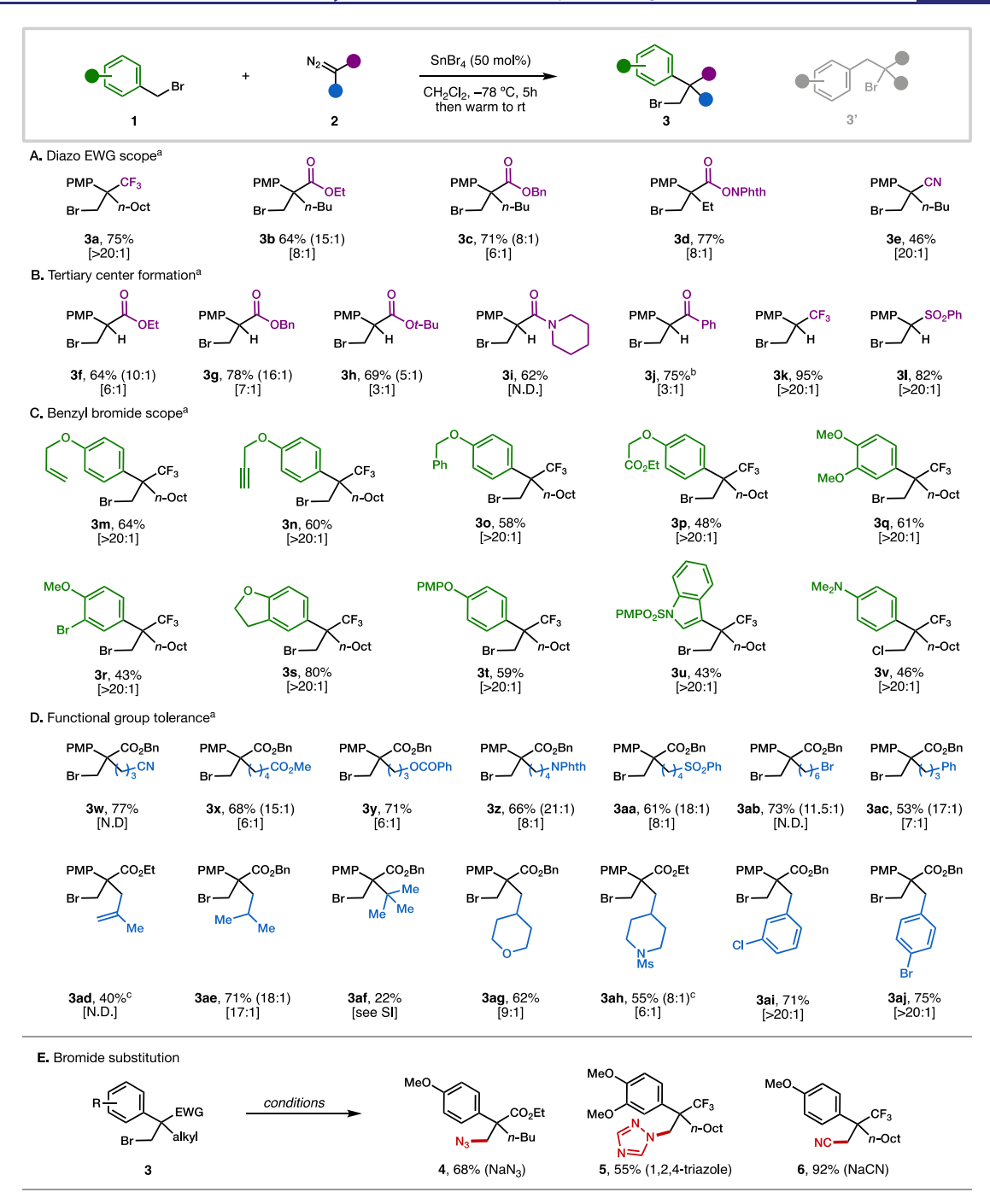
regioselectivity of phenonium ion opening was high (>20:1). Alkoxy substituents such as allyl (3m), propargyl (3n), benzyl (3o), and alkyl ester (3p) all deliver the desired products in good yields. Disubstituted arenes containing veratrole (3q) as well as 3-bromo and 4-methoxy (3r) motifs were tolerated. A dihydrobenzofuran derivative worked well (3s), and incorporation of an aryl ether is possible (3t). A rare example of an "indolyl" phenonium ion was demonstrated through use of a 3-bromomethylindole derivative (3u), <sup>18</sup> and a 4-dimethylaminosubstituted benzyl chloride afforded chloride 3v in acceptable yield. Here, SnCl<sub>4</sub> was employed as the catalyst to avoid halogen crossover. Under these conditions, the use of benzyl bromide itself resulted in no reaction and recovered bromide (vide infra). <sup>19</sup>

Next, attention was turned to exploring the functional group tolerance of the reaction with respect to the alkyl substituent on the diazo derivative (Figure 2D).20 Here, benzyl diazoacetate derivatives were employed to facilitate substrate synthesis and handling. Many different functional groups were tolerated in this reaction, including nitrile (3w), ester (3x, 3y), phthalimide-protected amine (3z), sulfone (3aa), and bromide (3ab). A pendant phenyl ring was tolerated (3ac), and an allylsubstituted diazo afforded the desired product 3ad in modest yield. A diazo derived from the amino acid leucine also worked well (3ae). Remarkably, use of a tert-leucine-derived diazo compound afforded 3af which contains vicinal quaternary centers. The modest yield of this reaction (22%) results from a competitive methyl shift at the stage of phenonium ion formation (see the Supporting Information for details). Saturated heterocycles such as a tetrahydropyran and piperidine—commonly found in medicinally relevant compounds—could be incorporated in the diazo starting material and afforded the desired products (3ag, 3ah) in good yield. Use of benzyl-substituted diazo compounds opens the possibility of competitive aryl migration at the stage of the putative alkyl diazonium C (see Figure 1C). In both cases, the reaction proceeds in high yield, and the more electron-rich arene migrated selectively (3ai, 3aj).<sup>21</sup>

One enabling feature of this reaction is the retention of the alkyl bromide as a functional handle for further manipulation.

For example, substitution of the bromide with azide delivers  $\beta^{2,2}$ -amino acid derivative 4 in 68% yield (Figure 2E). Displacement with 1,2,4-triazole gave 5 in 55% yield. <sup>23</sup> 1,2,4-Triazoles are emerging as privileged scaffolds in medicinal chemistry<sup>24</sup> and also represent a core component of many agrochemical compounds (e.g., fenbuconazole, Figure 1D). Use of cyanide as the nucleophile afforded nitrile 6 in 92% yield.

Quantum chemical calculations (\omegaB97X-D/def2-QZVPP//  $\omega$ B97X-D/6-31+G(d,p) with an SMD description of dichloromethane) were used to study the multistep mechanism between 4-methoxybenzyl bromide and benzyl 2-diazobutanoate (as a model substrate) catalyzed by SnBr<sub>4</sub> (Figure 3A).<sup>25</sup> The initial nucleophilic displacement to form Int-II is computed to proceed most favorably in an S<sub>N</sub>1 fashion, with a barrier height of 18.5 kcal mol<sup>-1</sup> for TS-II (vs 29.7 kcal mol<sup>-1</sup> for the uncatalyzed S<sub>N</sub>2 pathway). This is the rate-determining step, for which lower barriers are obtained with electron-rich benzyl bromide derivatives (Figure 3B). Coordination of the bromide and Lewis acid results in a SnBr<sub>5</sub><sup>-</sup> leaving group in TS-I. After TS-II is crossed, the sequential loss of dinitrogen and phenonium ion formation proceeds through separate C-N breaking (TS-III) and C-C forming (TS-IV) TSs in a highly exergonic fashion ( $G_{rel} = -32.3 \text{ kcal mol}^{-1}$ ) to produce the phenonium Int-IV. The intervening intermediates, alkyl diazonium Int-II and tertiary carbocation Int-III, exist as local potential energy minima with extremely small exit barriers of just 0.3 and 2.0 kcal mol<sup>-1</sup>, respectively. Compared to phenonium formation, competing 1,2-hydride shifts (TS-VI and TS-VII) have higher barriers of 3.4-3.6 kcal mol<sup>-1</sup>. On the basis of these small barrier heights, we expect Int-II and Int-III to be short-lived, potentially preventing equilibration of atomic motions and the surrounding solvent, which limits the applicability of transition-state theory (TST).<sup>26</sup> We therefore initiated quasi-classical molecular dynamics trajectories<sup>27</sup> in the region of TS-II. Many of these trajectories evolved to phenonium Int-IV, passing through Int-II with an extremely short average lifetime (262 fs, only a few complete C-N vibrations occurred in many trajectories)<sup>28</sup> and Int-III, which had a longer lifetime of 439 fs, confirming the existence of



a Isolated yield of 3 quoted. The ratio of 3:3' in isolated material is given in parentheses. The ratio of 3:3' in the crude reaction mixture is given in brackets.

Figure 2. Reaction scope and demonstration of product utility.

dynamic intermediates. Although the potential energy surface is formally stepwise, we observed high fidelity transfer of stereochemical information from the starting material through to the phenonium configuration in MD trajectories that followed the main pathway.<sup>29</sup>

Regioselectivity is determined by nucleophilic phenonium opening via TS-V (Figure 3A). Nucleophilic attack by the pentavalent  $\mathrm{SnBr_5}^-$  anion is energetically favored over the free bromide anion by over 4 kcal  $\mathrm{mol}^{-1}$  for TS-V-A (see the Supporting Information, Figure S5) and C–Br formation occurs irreversibly ( $\Delta G = -16.4$  or -17.3 kcal  $\mathrm{mol}^{-1}$ ). The fleeting intermediacy of acyclic Int-III and the much greater

stability of Int-IV mean that direct addition of bromide before phenonium formation is unlikely. The direct trapping of tertiary carbocation (Int-III) by  $SnBr_5^-$  is less favorable than phenonium formation by 1.5 kcal  $mol^{-1}$  (see Figure S3). This minor pathway could nonetheless provide a direct route to product B in addition to the opening of phenonium through TS-V-B. We then compared DFT-computed selectivities arising from the competing TSs for seven substrate combinations with experiment. The trends and regioselectivities were well reproduced (see Figure S7). Compared to the favored ring-opening pathway TS-V-A, which involves nucleophilic attack at the methylene group, the less-favorable

<sup>&</sup>lt;sup>b</sup> In situ yield quoted <sup>c</sup> The ethyl ester was employed.

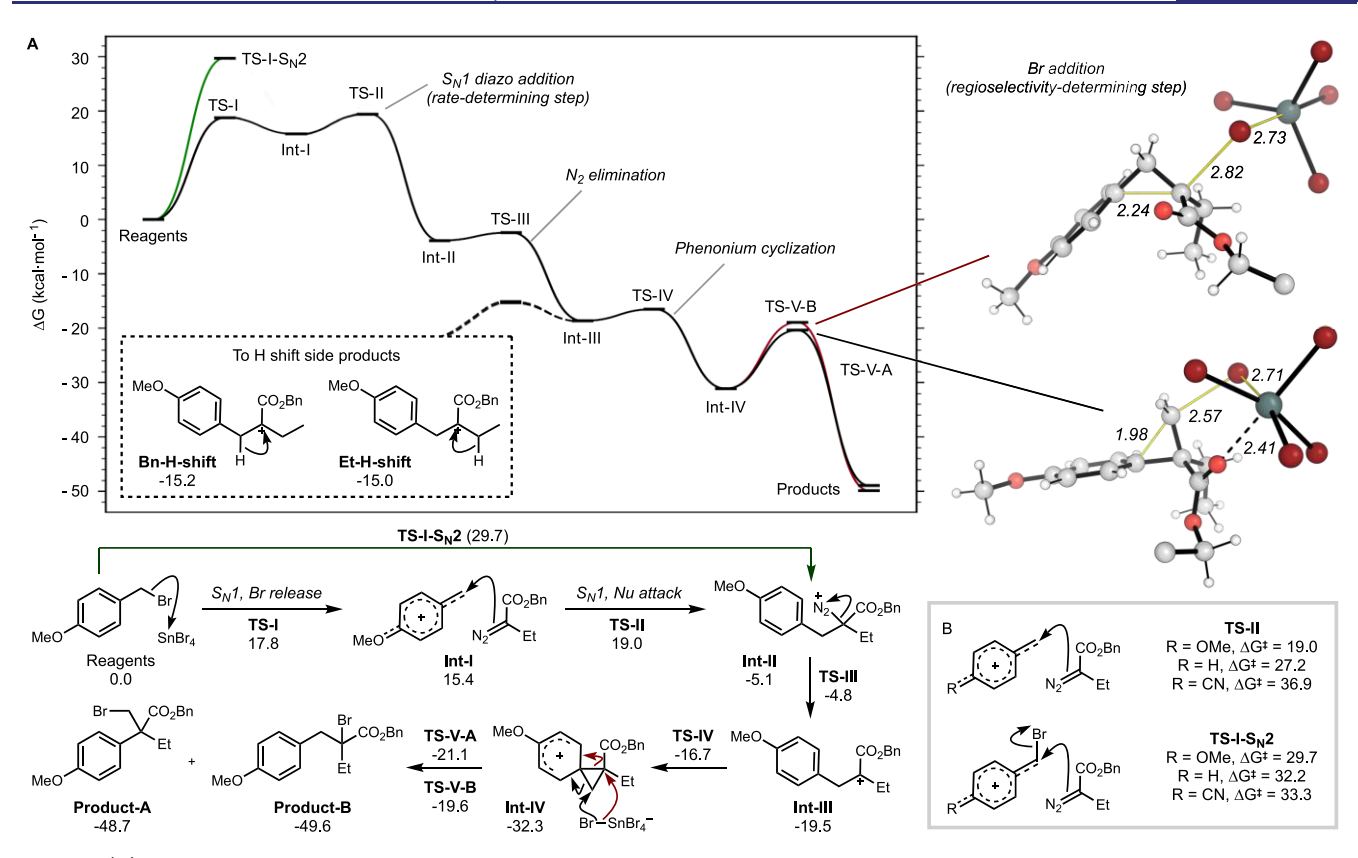


Figure 3. (A) Computed Gibbs energy profile at -78 °C, 1 M standard state. DFT calculations were performed at the  $\omega$ B97X-D/def2-QZVPP// $\omega$ B97X-D/6-31+G(d,p) (def2-SVPD for Sn during optimization) level of theory. Ph groups are omitted for clarity. (B) Relative energies of diazo addition to benzyl bromide derivatives.

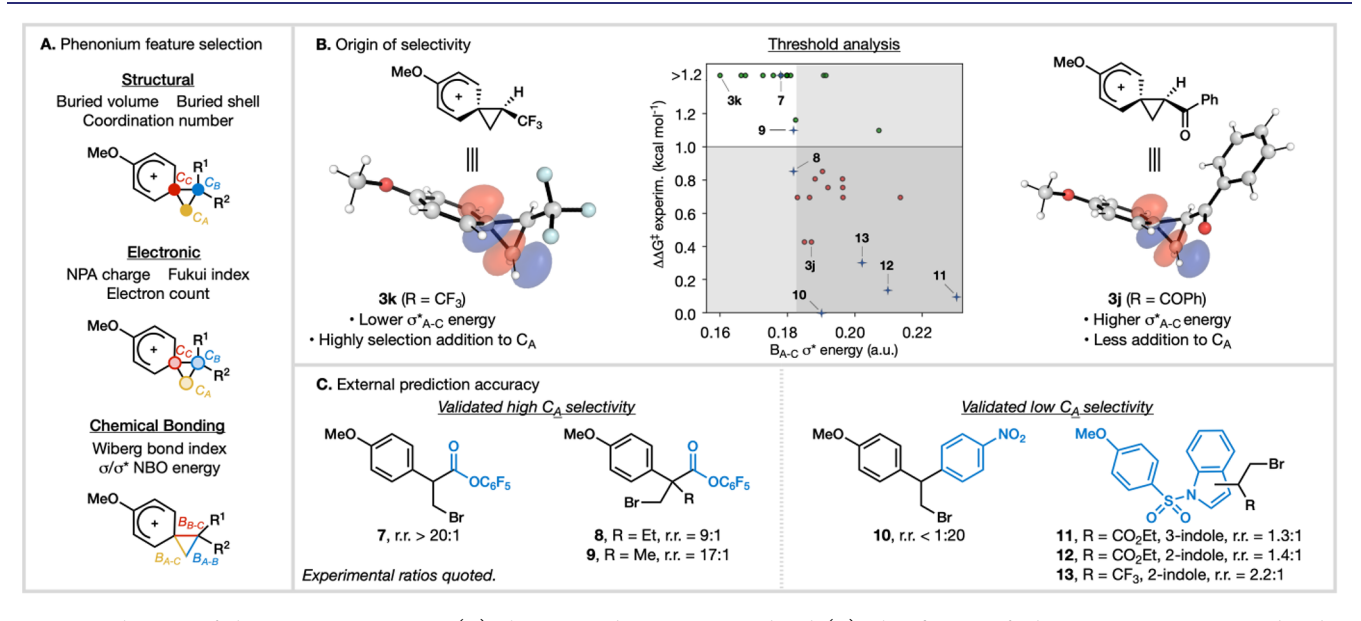


Figure 4. Selectivity of phenonium ion opening. (A) Phenonium descriptors considered. (B) Classification of selectivity using  $C_A - C_C$  antibonding energy establishing a threshold value. (C) Experimental validation of the model.

TS-V-B requires greater elongation of the cyclic C–C bond (by 0.26 Å) to reach the TS, which is looser and more "exploded" than its more stable counterpart.<sup>30</sup> Similarly, greater C–C bond breaking in the minor vs major TS was observed for all substrates considered.

To further investigate the relationship between structure of the phenonium intermediate and experimentally observed regioselectivity, we performed a statistical analysis. Structural, electronic, and chemical bonding parameters of 25 phenonium intermediates were selected as key descriptors (Figure 4A and Figure S9). Inspired by Sigman and Doyle's application of a single-node decision tree to infer mechanistic information, we sought to identify a single descriptor able to function as a classifier separating highly regionselective from unselective substrates.<sup>31</sup> The use of a classification model, rather than (non)linear regression model, is also particularly well-suited

here since several substrates produce a single regioisomer (>20:1), preventing an exact value of  $\Delta\Delta G^\ddagger$  being assigned. We therefore split the experimental data into high and low selectivity values, with an experimental r.r. of 13:1 ( $\Delta\Delta G^\ddagger=1$  kcal mol $^{-1}$ ) serving as this cutoff. We identified a chemical bonding feature, the energy of the natural  $C_A-C_C$   $\sigma^*$  orbital, performed best and allowed us to identify a "threshold" energy (0.183 au) below which all substrates react with high regioselectivity (Figure 4B). Phenonium ions with  $C_A-C_C$   $\sigma^*$  energies below this threshold universally give experimental selectivities >13:1, while of those with energies above this threshold 11/14 (79%) give low selectivities. This is the bond cleaved irreversibly in the transition structure, leading to the formation of the major (i.e., homologated) regioisomer.

To validate this model, seven out-of-sample substrates bearing different substituents to those used during training were designed theoretically with predicted selectivities ranging from high (7-9) to low (10-13). These predictions generated by the classifier were consistent with the experimental results (Figure 4C).

In conclusion, we report a homologation reaction of benzyl bromides with diazo derivatives. This reaction exploits the classical reactivity of benzyl halides (as electrophiles) and aromatic rings (as nucleophiles) to achieve formal insertion of a diazo into the  $C(sp^2)-C(sp^3)$  bond. Computational analysis of the reaction coordinate revealed a rate-determining  $S_N1$  mechanism for the initial C-C bond formation followed by a cascading sequence of cationic intermediates leading to a phenonium ion. Insights into the regioselectivity of phenonium ion opening were gained and enabled *a priori* prediction of reaction outcomes for new substrate combinations. Overall, this work provides a modular method for constructing acyclic, benzylic quaternary centers from readily accessible starting materials which we anticipate may find utility in drug discovery programs.

### ASSOCIATED CONTENT

#### Supporting Information

The Supporting Information is available free of charge at https://pubs.acs.org/doi/10.1021/jacs.1c11503.

Experimental procedures, characterization data for novel compounds, crystallographic analysis, and computational details (PDF)

# **Accession Codes**

CCDC 2101216 contains the supplementary crystallographic data for this paper. These data can be obtained free of charge via <a href="www.ccdc.cam.ac.uk/data\_request/cif">www.ccdc.cam.ac.uk/data\_request/cif</a>, or by emailing data\_request@ccdc.cam.ac.uk, or by contacting The Cambridge Crystallographic Data Centre, 12 Union Road, Cambridge CB2 1EZ, UK; fax: +44 1223 336033.

#### AUTHOR INFORMATION

# **Corresponding Authors**

Nicholas J. Race — Department of Chemistry, University of Minnesota—Twin Cities, Minneapolis, Minnesota 55455, United States; Orcid.org/0000-0002-0755-1724; Email: nrace@umn.edu

Robert S. Paton — Department of Chemistry, Colorado State University, Fort Collins, Colorado 80523, United States; orcid.org/0000-0002-0104-4166; Email: robert.paton@colostate.edu

#### Authors

Atanu Modak – Department of Chemistry, University of Minnesota—Twin Cities, Minneapolis, Minnesota 55455, United States; orcid.org/0000-0002-1625-9733

Juan V. Alegre-Requena – Department of Chemistry, Colorado State University, Fort Collins, Colorado 80523, United States

Louis de Lescure — Department of Chemistry, Colorado State University, Fort Collins, Colorado 80523, United States

Kathryn J. Rynders — Department of Chemistry, University of Minnesota—Twin Cities, Minneapolis, Minnesota 55455, United States

Complete contact information is available at: https://pubs.acs.org/10.1021/jacs.1c11503

#### **Funding**

N.J.R. acknowledges financial support from the University of Minnesota, the American Chemical Society Petroleum Research Fund (PRF 60782-DNI1), and the National Institute of General Medical Sciences of the National Institutes of Health under Award R35GM137920. N.J.R. also acknowledges the NIH Shared Instrumentation Grant S10OD011952. R.S.P. acknowledges financial support from the National Science Foundation under Grant 1955876 and the RMACC Summit supercomputer, supported by the National Science Foundation (ACI-1532235 and ACI-1532236), the University of Colorado Boulder and Colorado State University, and the Extreme Science and Engineering Discovery Environment (XSEDE) through allocation TG-CHE180056.

#### **Notes**

The authors declare the following competing financial interest(s): N.J.R. and A.M. have filed a provisional patent on chemistry disclosed in this manuscript.

# ■ ACKNOWLEDGMENTS

Dr. Victor G. Young, Jr. (UMN), is acknowledged for assistance with X-ray crystallographic analysis of compound 3d.

# **■** REFERENCES

- (1) Corey, E. J.; Cheng, X. M. The Logic of Chemical Synthesis; Wiley: 1989
- (2) Dakka, J.; Sasson, Y. Bromination of  $\alpha$ -substituted alkylbenzenes: synthesis of (p-bromophenyl)acetylene. *J. Org. Chem.* **1989**, *54*, 3224–3226.
- (3) (a) Tambar, U. K.; Stoltz, B. M. The Direct Acyl-Alkylation of Arynes. J. Am. Chem. Soc. 2005, 127, 5340–5341. (b) Hashimoto, T.; Naganawa, Y.; Maruoka, K. Brønsted Acid-Catalyzed Insertion of Aryldiazoacetates to sp<sup>2</sup> Carbon–CHO Bond: Facile Construction of Chiral All-Carbon Quaternary Center. J. Am. Chem. Soc. 2008, 130, 2434–2435.
- (4) Direct C–C bond insertion reactions typically involve transition metal catalysis, directing groups, and strained C–C bonds. See: (a) Souillart, L.; Cramer, N. Catalytic C–C Bond Activations via Oxidative Addition to Transition Metals. *Chem. Rev.* 2015, 115, 9410–9464. (b) Fumagalli, G.; Stanton, S.; Bower, J. F. Recent Methodologies That Exploit C–C Single-Bond Cleavage of Strained Ring Systems by Transition Metal Complexes. *Chem. Rev.* 2017, 117, 9404–9432. (c) Xia, Y.; Dong, G. Temporary or removable directing groups enable activation of unstrained C–C bonds. *Nat. Rev. Chem.* 2020, 4, 600–614.
- (5) For a recent related reaction involving benzhydryl acetates and ethyl diazoacetate, see: Wang, F.; Yi, J.; Nishimoto, Y.; Yasuda, M. Homologation of Alkyl Acetates, Alkyl Ethers, Acetals, and Ketals by

Formal Insertion of Diazo Compounds into a Carbon–Carbon Bond. *Synthesis* **2021**, *53*, 4004–4019.

- (6) (a) Ford, A.; Miel, H.; Ring, A.; Slattery, C. N.; Maguire, A. R.; McKervey, M. A. Modern Organic Synthesis with α-Diazocarbonyl Compounds. *Chem. Rev.* **2015**, *115*, 9981–10080. (b) Candeias, N. R.; Paterna, R.; Gois, P. M. P. Homologation Reaction of Ketones with Diazo Compounds. *Chem. Rev.* **2016**, *116*, 2937–2981. (c) Guttenberger, N.; Breinbauer, R. CH and CC bond insertion reactions of diazo compounds into aldehydes. *Tetrahedron* **2017**, *73*, 6815–6829. (d) Green, S. P.; Wheelhouse, K. M.; Payne, A. D.; Hallett, J. P.; Miller, P. W.; Bull, J. A. Thermal Stability and Explosive Hazard Assessment of Diazo Compounds and Diazo Transfer Reagents. *Org. Process Res. Dev.* **2020**, *24*, 67–84.
- (7) Bug, T.; Hartnagel, M.; Schlierf, C.; Mayr, H. How Nucleophilic Are Diazo Compounds? *Chem. Eur. J.* **2003**, *9*, 4068–4076.
- (8) Cram, D. J. Phenonium Ions as Discrete Intermediates in Certain Wagner-Meerwein Rearrangements. *J. Am. Chem. Soc.* **1964**, 86, 3767–3772.
- (9) For recent examples of phenonium ions in synthesis, see: (a) Li, X.; Li, C.; Zhang, W.; Lu, X.; Han, S.; Hong, R. Highly Stereoselective 7-Endo-Trig/Ring Contraction Cascade To Construct Pyrrolo[1,2a]quinoline Derivatives. Org. Lett. 2010, 12, 1696-1699. (b) Protti, S.; Dondi, D.; Mella, M.; Fagnoni, M.; Albini, A. Looking for a Paradigm for the Reactivity of Phenonium Ions. Eur. J. Org. Chem. 2011, 2011, 3229-3237. (c) Li, J.; Bauer, A.; Di Mauro, G.; Maulide, N. α-Arylation of Carbonyl Compounds through Oxidative C-C Bond Activation. Angew. Chem., Int. Ed. 2019, 58, 9816-9819. (d) Sharma, H. A.; Mennie, K. M.; Kwan, E. E.; Jacobsen, E. N. Enantioselective Aryl-Iodide-Catalyzed Wagner-Meerwein Rearrangements. J. Am. Chem. Soc. 2020, 142, 16090-16096. (e) Xu, S.; Holst, H. M.; McGuire, S. B.; Race, N. J. Reagent Control Enables Selective and Regiodivergent Opening of Unsymmetrical Phenonium Ions. J. Am. Chem. Soc. 2020, 142, 8090-8096. (f) Martins, B. S.; Kaiser, D.; Bauer, A.; Tiefenbrunner, I.; Maulide, N. Formal Enone  $\alpha$ -Arylation via I(III)-Mediated Aryl Migration/Elimination. Org. Lett. 2021, 23, 2094-2098.
- (10) Kang, K.-T.; Kim, S. T.; Hwang, G.-S.; Ryu, D. H. Catalytic Enantioselective Protonation/Nucleophilic Addition of Diazoesters with Chiral Oxazaborolidinium Ion Activated Carboxylic Acids. *Angew. Chem., Int. Ed.* **2017**, *56*, 3977–3981.
- (11) (a) Lovering, F.; Bikker, J.; Humblet, C. Escape from Flatland: Increasing Saturation as an Approach to Improving Clinical Success. *J. Med. Chem.* **2009**, *52*, *6752*–*6756*. (b) Lovering, F. Escape From Flatland 2: Complexity and Promiscuity. *MedChemComm* **2013**, *4*, 515–519.
- (12) (a) Ling, T.; Rivas, F. All-carbon quaternary centers in natural products and medicinal chemistry: recent advances. *Tetrahedron* **2016**, 72, 6729–6777. (b) Talele, T. T. Opportunities for Tapping into Three-Dimensional Chemical Space through a Quaternary Carbon. *J. Med. Chem.* **2020**, *63*, 13291–13315.
- (13) For select examples of recent methods that generate acyclic, quaternary benzylic centers, see: (a) Fillion, E.; Wilsily, A. Asymmetric Synthesis of All-Carbon Benzylic Quaternary Stereocenters via Cu-Catalyzed Conjugate Addition of Dialkylzinc Reagents to 5-(1-Arylalkylidene) Meldrum's Acids. J. Am. Chem. Soc. 2006, 128, 2774-2775. (b) Bonet, A.; Odachowski, M.; Leonori, D.; Essafi, S.; Aggarwal, V. K. Enantiospecific sp<sup>2</sup>-sp<sup>3</sup> coupling of secondary and tertiary boronic esters. Nat. Chem. 2014, 6, 584-589. (c) Marek, I.; Minko, Y.; Pasco, M.; Mejuch, T.; Gilboa, N.; Chechik, H.; Das, J. P. All-Carbon Quaternary Stereogenic Centers in Acyclic Systems through the Creation of Several C-C Bonds per Chemical Step. J. Am. Chem. Soc. 2014, 136, 2682-2694. (d) Huang, C.-Y.; Doyle, A. G. Electron-Deficient Olefin Ligands Enable Generation of Quaternary Carbons by Ni-Catalyzed Cross-Coupling. J. Am. Chem. Soc. 2015, 137, 5638-5641. (e) Starkov, P.; Moore, J. T.; Duquette, D. C.; Stoltz, B. M.; Marek, I. Enantioselective Construction of Acyclic Quaternary Carbon Stereocenters: Palladium-Catalyzed Decarboxylative Allylic Alkylation of Fully Substituted Amide Enolates. J. Am. Chem. Soc. 2017, 139, 9615-9620. (f) Yoon, H.; Marchese, A. D.;

- Lautens, M. Carboiodination Catalyzed by Nickel. *J. Am. Chem. Soc.* **2018**, 140, 10950–10954. (g) Zhang, H.-H.; Zhao, J.-J.; Yu, S. Enantioselective Allylic Alkylation with 4-Alkyl-1,4-dihydro-pyridines Enabled by Photoredox/Palladium Cocatalysis. *J. Am. Chem. Soc.* **2018**, 140, 16914–16919. (h) Wendlandt, A. E.; Vangal, P.; Jacobsen, E. N. Quaternary Stereocentres via an Enantioconvergent Catalytic SN1 Reaction. *Nature* **2018**, 556, 447–451. (i) Li, Y.; Han, J.; Luo, H.; An, Q.; Cao, X.-P.; Li, B. Access to Benzylic Quaternary Carbons from Aromatic Ketones. *Org. Lett.* **2019**, 21, 6050–6053.
- (14) For reviews on the construction of quaternary centers, see: (a) Christoffers, J.; Baro, A. Stereoselective Construction of Quaternary Stereocenters. Adv. Synth. Catal. 2005, 347, 1473–1482. (b) Quasdorf, K. W.; Overman, L. E. Catalytic enantioselective synthesis of quaternary carbon stereocentres. Nature 2014, 516, 181–191. (c) Feng, J.; Holmes, M.; Krische, M. J. Acyclic Quaternary Carbon Stereocenters via Enantioselective Transition Metal Catalysis. Chem. Rev. 2017, 117, 12564–12580. (d) Süsse, L.; Stoltz, B. M. Enantioselective Formation of Quaternary Centers by Allylic Alkylation with First-Row Transition-Metal Catalysts. Chem. Rev. 2021, 121, 4084–4099. (e) Xue, W.; Jia, X.; Wang, X.; Tao, X.; Yin, Z.; Gong, H. Nickel-catalyzed formation of quaternary carbon centers using tertiary alkyl electrophiles. Chem. Soc. Rev. 2021, 50, 4162–4184.
- (15) (a) Gillis, E. P.; Eastman, K. J.; Hill, M. D.; Donnelly, D. J.; Meanwell, N. A. Applications of Fluorine in Medicinal Chemistry. J. Med. Chem. 2015, 58, 8315–8359. (b) Zhou, Y.; Wang, J.; Gu, Z.; Wang, S.; Zhu, W.; Aceña, J. L.; Soloshonok, V. A.; Izawa, K.; Liu, H. Next Generation of Fluorine-Containing Pharmaceuticals, Compounds Currently in Phase II–III Clinical Trials of Major Pharmaceutical Companies: New Structural Trends and Therapeutic Areas. Chem. Rev. 2016, 116, 422–518. (c) Johnson, B. M.; Shu, Y.-Z.; Zhuo, X.; Meanwell, N. A. Metabolic and Pharmaceutical Aspects of Fluorinated Compounds. J. Med. Chem. 2020, 63, 6315–6386.
- (16) (a) Holmes, M.; Nguyen, K. D.; Schwartz, L. A.; Luong, T.; Krische, M. J. Enantioselective Formation of CF<sub>3</sub>-Bearing All-Carbon Quaternary Stereocenters via C–H Functionalization of Methanol: Iridium Catalyzed Allene Hydrohydroxymethylation. *J. Am. Chem. Soc.* 2017, 139, 8114–8117. (b) Mykhailiuk, P. K. 2,2,2-Trifluorodiazoethane (CF<sub>3</sub>CHN<sub>2</sub>): A Long Journey since 1943. *Chem. Rev.* 2020, 120, 12718–12755.
- (17) Lower catalyst loadings resulted in lower yields. For more details on the optimization see Table S1 in the Supporting Information.
- (18) Lang, J. H.; Jones, P. G.; Lindel, T. Total Synthesis of the Marine Natural Product Hemiasterlin by Organocatalyzed  $\alpha$ -Hydrazination. *Chem. Eur. J.* **2017**, *23*, 12714–12717.
- (19) The reaction of PMBCl and diazo 2 with  $SnCl_4$  as catalyst afforded the chloride derivative of 3a in 70% in situ yield. Benzyl iodides were not investigated in this chemistry due to their anticipated instability.
- (20) The reaction of phenyl diazoacetate with *p*-methoxybenzyl bromide resulted in addition of PMB and Br to the diazo carbon without aryl migration. A related reaction involving benzyl fluorides and aryl diazoacetates was reported while our manuscript was under review: Wang, F.; Nishimoto, Y.; Yasuda, M. Insertion of Diazo Esters into C–F Bonds toward Diastereoselective One-Carbon Elongation of Benzylic Fluorides: Unprecedented BF<sub>3</sub> Catalysis with C–F Bond Cleavage and Re-formation, *J. Am. Chem. Soc.* **2021**, .
- (21) Curtin, D. Y.; Crew, M. C. Migration Ratios in the Rearrangement of 2-Amino-1,1-diarylethanols. *J. Am. Chem. Soc.* **1954**, 76, 3719–3722.
- (22) Abele, S.; Seebach, D. Preparation of Achiral and of Enantiopure Geminally Disubstituted  $\beta$ -Amino Acids for  $\beta$ -Peptide Synthesis. *Eur. J. Org. Chem.* **2000**, 2000, 1–15.
- (23) Bulger, P. G.; Cottrell, I. F.; Cowden, C. J.; Davies, A. J.; Dolling, U.-H. An investigation into the alkylation of 1,2,4-triazole. *Tetrahedron Lett.* **2000**, *41*, 1297–1301.
- (24) Aggarwal, R.; Sumran, G. An insight on medicinal attributes of 1,2,4-triazoles. Eur. J. Med. Chem. 2020, 205, 112652.

- (25) (a) All calculations were performed with Gaussian 16, Rev. C.01; Gaussian, Inc.: Wallingford, CT, 2016, and with NBO, ver. 7.0. Glendening, E. D.; Badenhoop, J. K.; Reed, A. E.; Carpenter, J. E.; Bohmann, J. A.; Morales, C. M.; Karafiloglou, P.; Landis, C. R.; Weinhold, F. Theoretical Chemistry Institute, University of Wisconsin, Madison, WI, 2013. Full computational details are provided as Supporting Information. (b) Luchini, G.; Alegre-Requena, J. V.; Funes-Ardoiz, I.; Paton, R. S. GoodVibes: Automated Thermochemistry for Heterogeneous Computational Chemistry Data. F1000Research 2020, 9, 291.
- (26) (a) Oyola, Y.; Singleton, D. A. Dynamics and the Failure of Transition State Theory in Alkene Hydroboration. *J. Am. Chem. Soc.* **2009**, *131*, 3130–3131. (b) Chen, Z.; Nieves-Quinones, Y.; Waas, J. R.; Singleton, D. A. Isotope Effects, Dynamic Matching, and Solvent Dynamics in a Wittig Reaction. Betaines as Bypassed Intermediates. *J. Am. Chem. Soc.* **2014**, *136*, 13122–13125.
- (27) Kwan, E. E.; Liu, R. Y. Enhancing NMR Prediction for Organic Compounds Using Molecular Dynamics. *J. Chem. Theory Comput.* **2015**, *11*, 5083–5089.
- (28) Black, K.; Liu, P.; Xu, L.; Doubleday, C.; Houk, K. N. Dynamics, transition states, and timing of bond formation in Diels—Alder reactions. *Proc. Natl. Acad. Sci. U. S. A.* **2012**, *109*, 12860.
- (29) Ascough, D. M. H.; Duarte, F.; Paton, R. S. Stereospecific 1,3-H Transfer of Indenols Proceeds via Persistent Ion-Pairs Anchored by NH··· $\pi$  Interactions. *J. Am. Chem. Soc.* **2018**, *140*, 16740–16748.
- (30) Knier, B. L.; Jencks, W. P. Mechanism of reactions of N-(methoxymethyl)-N,N-dimethylanilinium ions with nucleophilic reagents. *J. Am. Chem. Soc.* **1980**, *102*, 6789–6798.
- (31) Newman-Stonebraker, S. H.; Smith, S. R.; Borowski, J. E.; Peters, E.; Gensch, T.; Johnson, H. C.; Sigman, M. S.; Doyle, A. G. Univariate classification of phosphine ligation state and reactivity in cross-coupling catalysis. *Science* **2021**, *374*, 301–308.